Nitroacetylene: Computed Heats of Formation and Analysis of Reaction Mechanisms with Vinyl Ethers

Peter Politzer,* Pat Lane, and Monica C. Concha

Department of Chemistry, University of New Orleans, New Orleans, Louisiana 70148

Received: October 30, 2003; In Final Form: January 7, 2004

The first synthesis of nitroacetylene was recently reported by Zhang et al. (Zhang, M.-X.; Eaton, P. E.; Steele, I.; Gilardi, R. *Synthesis* **2002**, 2013). They found it to react in a seemingly anomalous fashion with furan and with vinyl ethers, yielding nitrovinylisoxazoles. Mechanisms were proposed that would account for these unexpected products. We have investigated these mechanisms computationally in vinyl methyl ether at the B3PW91/6-311G(3df,2pd) level, calculating ΔH and the activation barrier for each of the 10 steps. Our results fully support the interpretation of Zhang et al. All of the steps were found to be exothermic and to have low barriers, between 1 and 14 kcal/mol. Using other computational procedures, we also determined the molecular geometry of nitroacetylene, its gas and liquid phase heats of formation, and its molecular surface electrostatic potential.

1. Introduction

Zhang et al. recently achieved the first synthesis of nitroacetylene (**1**).[1] This is viewed as the initial step in a possible route to octanitrocubane (**2**), via the tetramerization of dinitroacetylene (**3**), shown in eq 1:

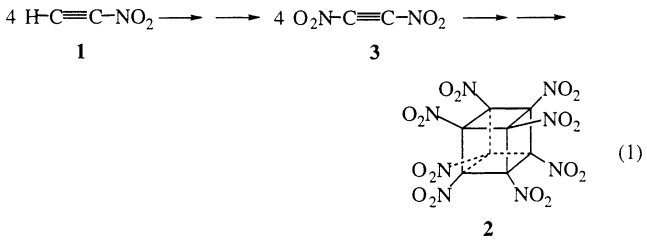

(1)

Octanitrocubane is potentially a very important high-performance energetic compound,[2−4] which was finally synthesized in 2000 after many years of effort.[5] For practical purposes, however, a more economical preparative procedure is needed, hence the interest in eq 1.

A two-step conversion of dinitroacetylene to octanitrocubane, **3** (4 equiv) ⟶⟶ **2**, has been investigated computationally at the Kohn−Sham B3P86/6-31G** level and was found to be thermodynamically feasible, $\Delta G = -99$ kcal/mol.[3] Unfortunately, dinitroacetylene is presently not known, nor, until recently, was nitroacetylene.

Zhang et al. made no attempt to isolate nitroacetylene, but they characterized it spectroscopically in solution (IR and NMR) and explored some of its chemistry.[1] They found that it reacts rapidly with nucleophiles and, as expected, behaves as a dienophile toward cyclopentadiene, giving the Diels−Alder adduct. Surprisingly, however, this did not occur with furan; instead of a Diels−Alder reaction, two isomeric nitroisoxazoles were obtained. In trying to understand this, Zhang et al. looked at the reactions of nitroacetylene with two vinyl ethers, **4** and **5**. In both instances, isomeric nitrovinylisoxazoles resulted; for example, **1** + **5** produced a mixture of **6a** and **6b**.

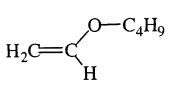

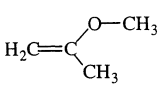

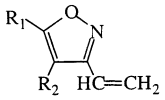

6a: R_1=H, R_2=NO_2
6b: R_1=NO_2, R_2=H

Zhang et al. have suggested two possible mechanisms to account for these observations, as shown in Scheme 1,[1] in which the vinyl ether is taken to be $H_2C{=}CH{-}OCH_3$ (**7**). The [4 + 2] cycloaddition **1** + **7** → **8** was proposed by analogy to the known behavior of nitroalkenes.[6] Zhang et al. anticipate that the strain in the resulting adduct **8** could lead to fragmentation, producing vinyl nitrile oxide **10**, which would undergo [3 + 2] cycloadditions with **1** to yield **6a** and **6b**. These could react with more **10** to give another pair of isomeric nitrovinylisoxazoles, **11a** and **11b**, which were among the products obtained from nitroacetylene plus vinyl butyl ether;[1] the structure of **11b** was established crystallographically.[1] Alternatively, **8** might add to **1**, forming **12a** and **12b**, which could split off an ester to give **6a** and **6b**. Zhang et al. speculate that either or both of these pathways could be involved in the reaction of nitroacetylene with a vinyl ether.

Our objectives in this computational study have been twofold: (a) to further characterize nitroacetylene itself, in terms of its gas and liquid phase heats of formation, its molecular geometry, and its molecular surface electrostatic potential, and (b) to determine the energetics, including activation barriers, of the various reaction steps in Scheme 1, to better assess the likelihood of the proposed mechanisms.

2. Physical Properties

2.1. Gas Phase Heat of Formation. We found the gas phase heat of formation of nitroacetylene by applying the definition

* To whom correspondence should be addressed. E-mail: ppolitze@uno.edu.

10.1021/jp031213o CCC: $27.50
Published on Web 03/18/2004

SCHEME 1

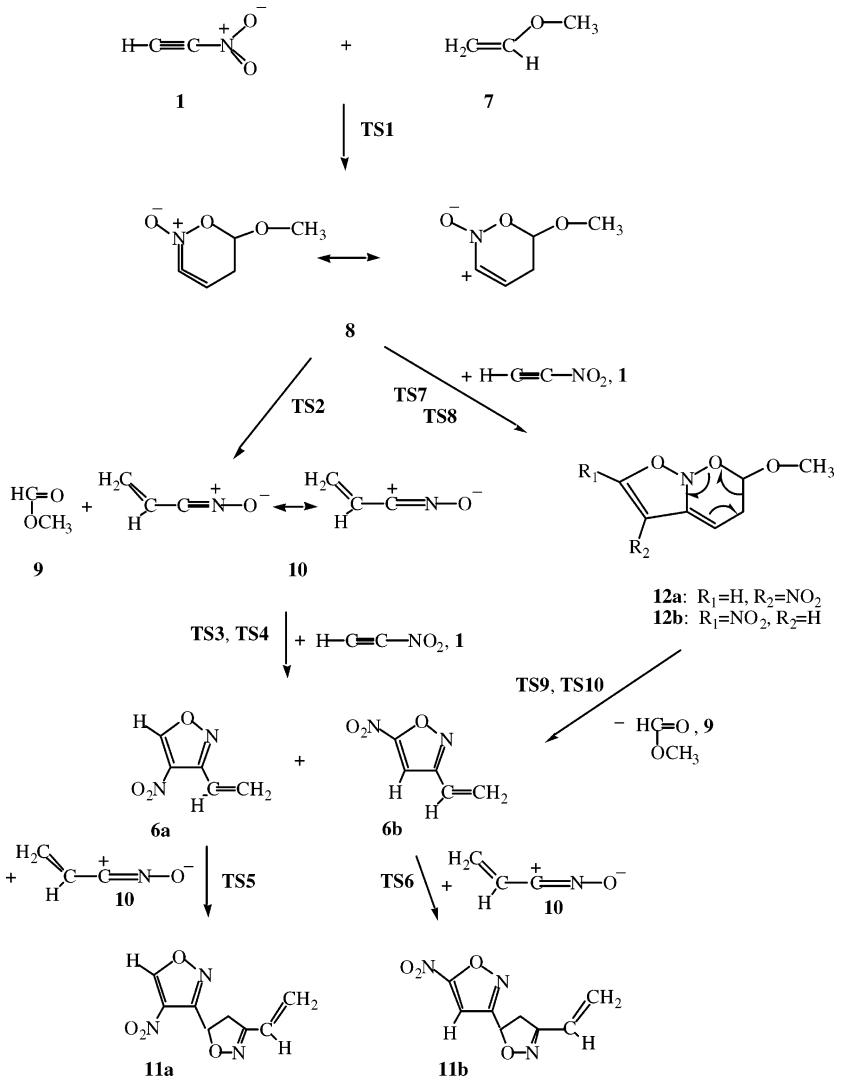

and calculating ΔH(298 K) for the following reaction:

$$2C(s) + {}^1/_2H_2(g) + {}^1/_2N_2(g) + O_2(g) \rightarrow H{-}C{\equiv}C{-}NO_2(g) \quad (2)$$

We used the Gaussian 98 code[7] and two composite *ab initio* procedures, the CBS-QB3,[8] which reproduces atomization energies with a mean absolute deviation from experiment of 0.58 kcal/mol, and the G3(MP2),[9] which gives heats of formation for substituted hydrocarbons with an average absolute deviation of 0.74 kcal/mol. After taking into account the sublimation energy of carbon, 171.29 kcal/mol,[10] we find the CBS-QB3 ΔH(298 K) for reaction 2 to be 67.8 kcal/mol, while the G3(MP2) one is 66.6 kcal/mol. Our predicted gas phase heat of formation for nitroacetylene is therefore 67 kcal/mol.

2.2. Liquid Phase Heat of Formation. Since Zhang et al. believe that the boiling point of nitroacetylene is between 60 and 100 °C,[1] its liquid heat of formation is more relevant than the gas phase value. ΔH_f(liquid) can be determined if the heat of vaporization is known:

$$\Delta H_f(\text{liquid}) = \Delta H_f(\text{gas}) - \Delta H_{vap} \quad (3)$$

We have shown, in a series of studies, that heats of vaporization,[11] as well as a variety of other condensed phase properties that depend on noncovalent interactions,[12−15] can be represented quantitatively in terms of certain statistically defined features of the electrostatic potentials, $V(\mathbf{r})$, on the molecules' surfaces. $V(\mathbf{r})$ is defined by

$$V(\mathbf{r}) = \sum_A \frac{Z_A}{|\mathbf{R}_A - \mathbf{r}|} - \int \frac{\rho(\mathbf{r}')\, d\mathbf{r}'}{|\mathbf{r}' - \mathbf{r}|} \quad (4)$$

in which Z_A is the charge on nucleus A, located at $\mathbf{R}_A$, and $\rho(\mathbf{r})$ is the molecular electronic density. For these purposes, $V(\mathbf{r})$ is evaluated on the molecular surface, which is taken to be the 0.001 electrons/b^3 contour of $\rho(\mathbf{r})$.[16] We found that ΔH_{vap} can be expressed by[11]

$$\Delta H_{vap} = \alpha A^{0.5} + \beta(\nu\sigma_{tot}^2)^{0.5} + \gamma \quad (5)$$

where A is the surface area and σ_{tot}^2 and ν are defined by eqs 6 and 7:

$$\sigma_{tot}^2 = \sigma_+^2 + \sigma_-^2 = \frac{1}{m}\sum_{i=1}^{m}[V_S^+(\mathbf{r}_i) - \bar{V}_S^+]^2 + \frac{1}{n}\sum_{j=1}^{n}[V_S^-(\mathbf{r}_j) - \bar{V}_S^-]^2 \quad (6)$$

$$\nu = \frac{\sigma_+^2\sigma_-^2}{[\sigma_{tot}^2]^2} \quad (7)$$

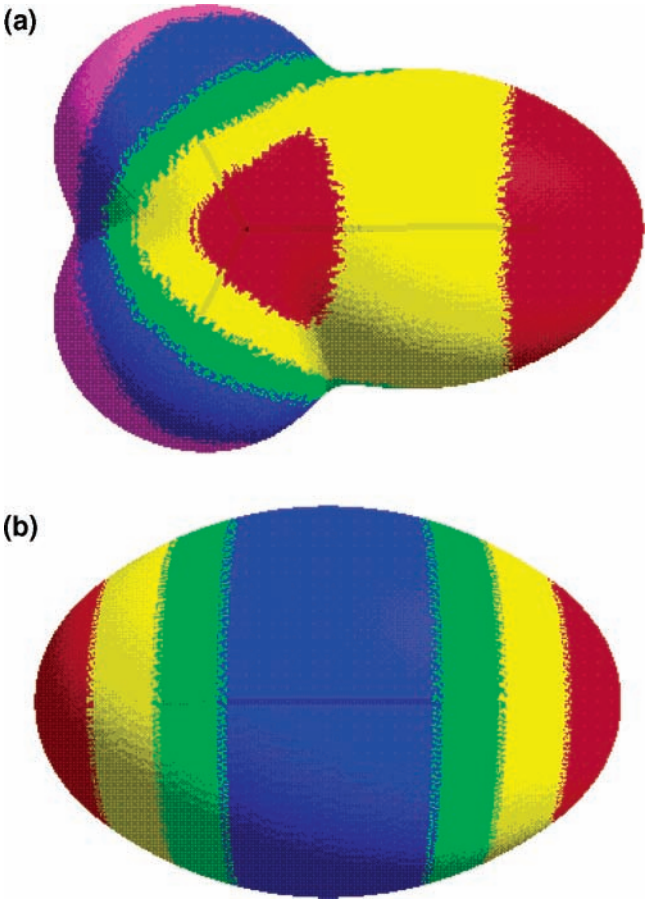

Figure 1. Computed HF/6-31G* electrostatic potentials on the molecular surfaces of (a) nitroacetylene and (b) acetylene. The surfaces are defined by the 0.001 electrons/b^3 contour of the electronic density. Color ranges, in kilocalories/mole: red, more positive than 15; yellow, between 15 and 0; green, between 0 and −10; blue, between −10 and −20; purple, more negative than −20.

TABLE 1: Computed Energetic Data for Scheme 1, in Hartrees

molecule[a]	E_{min}[b]	zero-pt + thermal term[c]	H(298 K)
1	−281.791 23	0.036 52	−281.754 71
7	−193.106 22	0.091 13	−193.015 09
TS1 (1 + 7 → 8)	−474.880 10	0.128 99	−474.751 11
8	−474.933 10	0.132 29	−474.800 81
TS2 (8 → 9 + 10)	−474.923 92	0.130 38	−474.793 54
9	−229.057 47	0.068 18	−228.989 29
10	−245.967 79	0.061 52	−245.906 27
TS3 (10 + 1 → 6a)	−527.741 83	0.098 63	−527.643 20
6a	−527.900 09	0.103 87	−527.796 22
TS4 (10 + 1 → 6b)	−527.738 27	0.098 53	−527.639 74
6b	−527.895 34	0.103 53	−527.791 81
TS5 (6a + 10 → 11a)	−773.849 15	0.165 99	−773.683 16
11a	−773.928 45	0.169 99	−773.758 46
TS6 (6b + 10 → 11b)	−773.842 61	0.165 63	−773.676 98
11b	−773.925 66	0.169 61	−773.756 05
TS7 (8 + 1 → 12a)	−756.722 75	0.169 49	−756.553 26
12a	−756.881 02	0.175 02	−756.706 00
TS8 (8 + 1 → 12b)	−756.723 58	0.169 84	−756.553 74
12b	−756.873 81	0.174 44	−756.699 37
TS9 (12a → 6a + 9)	−756.867 26	0.172 15	−756.695 11
TS10 (12b → 6b + 9)	−756.862 52	0.171 72	−756.690 80

[a] TS = transition state. The reaction in which it appears is shown in parentheses. [b] B3PW91/6-311G(3df,2pd) energy at 0 K, not including zero-point contribution. [c] B3PW91/6-31G(d) (see text).

$\bar{V}_S^+$ and $\bar{V}_S^-$ are the averages of the positive and negative values, $V_S^+(\mathbf{r}_i)$ and $V_S^-(\mathbf{r}_j)$, of $V(\mathbf{r})$ on the surface. We interpret

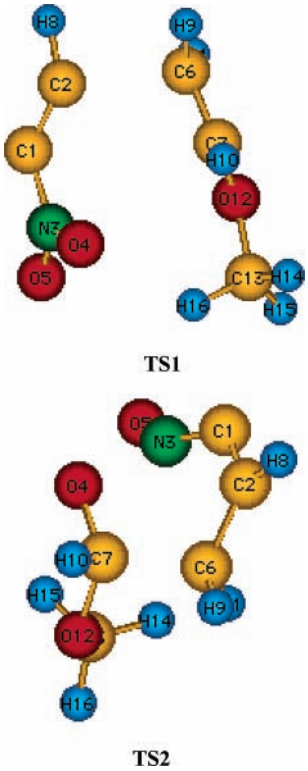

Figure 2. Computed B3PW91/6-311G(3df,2pd) structures of transition states **TS1** and **TS2**. In **TS1**, the distances between the atoms forming bonds are as follows: $C_2\cdots C_6$, 2.058 Å; $O_4\cdots C_7$, 2.948 Å. In **TS2**, the separations of the atoms between which bonds are being broken are as follows: $N_3\cdots O_4$, 1.756 Å; $C_6\cdots C_7$, 1.630 Å.

TABLE 2: Computed Reaction Energetics for Scheme 1, in Kilocalories per Mole

reaction	ΔH(298 K)	ΔH_{act}(298 K)
1 + 7 → TS1 → 8	−19.46	11.7
8 → TS2 → 9 + 10	−59.46	4.6
10 + 1 → TS3 → 6a	−84.9	11.2
10 + 1 → TS4 → 6b	−82.1	13.3
6a + 10 → TS5 → 11a	−35.1	12.1
6b + 10 → TS6 → 11b	−36.4	13.2
8 + 1 → TS7 → 12a	−94.4	1.42
8 + 1 → TS8 → 12b	−90.3	1.12
12a → TS9 → 6a + 9	−49.9	6.8
12b → TS10 → 6b + 9	−51.3	5.4

σ_{tot}^2 as indicative of the variability of the surface potential, $V_S(\mathbf{r})$, while ν measures the degree of balance between the strengths of the positive and negative regions. The parameters α, β, and γ were obtained by fitting eq 5 to the experimental heats of vaporization of a wide variety of liquids,[11] using a Hartree−Fock STO-5G $V_S(\mathbf{r})$. However, Rice et al. have recently reparametrized eq 5 at the density functional B3LYP/6-31G* level in terms of 21 organic energetic compounds, primarily nitro derivatives,[17] with an average absolute deviation of 1.3 kcal/mol.

Using the original eq 5 and HF/STO-5G data, we find ΔH_{vap} for nitroacetylene to be 8.4 kcal/mol; with the parameters of Rice et al. and a B3LYP/6-31G* $V_S(\mathbf{r})$, ΔH_{vap}(nitroacetylene) = 10.0 kcal/mol. Since the approach of Rice et al. is presumably the more accurate one for a nitro derivative, then we conclude, using eq 3, that

$$\Delta H_{vap}(\text{liquid nitroacetylene}) = 67 - 10 = 57 \text{ kcal/mol} \quad (8)$$

2.3. Molecular Geometry. The CBS-QB3 procedure that was used in calculating the gas phase heat of formation includes a

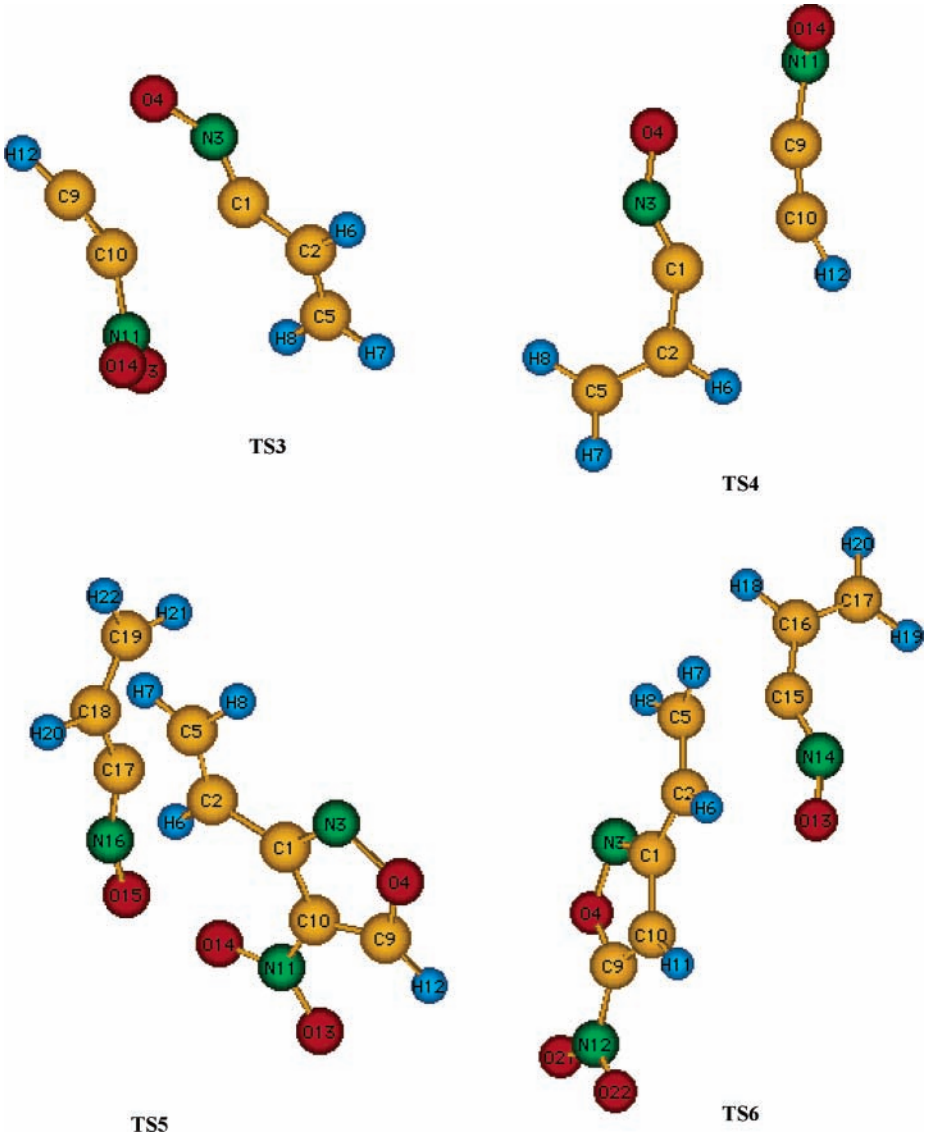

Figure 3. Computed B3PW91/6-311G(3df,2pd) structures of transition states **TS3**−**TS6**. The distances between the atoms forming bonds are as follows. **TS3**: $O_4 \cdots C_9$, 2.144 Å; $C_1 \cdots C_{10}$, 2.316 Å. **TS4**: $O_4 \cdots C_9$, 2.338 Å; $C_1 \cdots C_{10}$, 2.199 Å. **TS5**: $C_5 \cdots C_{17}$, 2.159 Å; $C_2 \cdots O_{15}$, 2.446 Å. **TS6**: $C_5 \cdots C_{15}$, 2.133 Å; $C_2 \cdots O_{13}$, 2.447 Å.

B3LYP/6-311G(2d,d,p) geometry optimization.[8] The predicted bond lengths in nitroacetylene are H—C, 1.064 Å; C—C, 1.197 Å; C—N, 1.403 Å; and N—O, 1.222 Å. The O—N—O angle is 126.8°. The C≡C and N—O distances and the O—N—O angle are quite typical,[18,19] while the C—H and C—N distances show the significant shortening that characterizes single bonds adjacent to multiple bonds.[20,21]

3. Chemical Reactive Behavior

3.1. Molecular Surface Electrostatic Potential. Zhang et al. assume that the nitroacetylene triple bond is "extremely electron deficient" and thus vulnerable to nucleophilic attack.[1] We have confirmed this by plotting the HF/6-31G* electrostatic potential, $V(\mathbf{r})$, (eq 4) on the molecular surface (as defined by the 0.001 electrons/b^3 contour of the electronic density[16]). This is shown in Figure 1a. To put it into perspective, it should be compared to $V(\mathbf{r})$ on the surface of unsubstituted acetylene (Figure 1b). (For earlier two-dimensional plots of $V(\mathbf{r})$ for acetylene and nitroacetylene, see ref 22.) Acetylene has a strong negative region associated with the triple bond, that gradually becomes positive as the hydrogens are approached. The negative triple bond potential is essentially completely gone in nitroacetylene; the only negative region is that due to the nitro oxygens. The hydrogen is now much more positive, and a particularly interesting feature is the strongly positive potential above the C−NO_2 bond. This has been observed earlier in nitro derivatives of a variety of molecules[22−25] and represents a possible channel for the approach of a nucleophile.[26]

3.2. Reaction with Vinyl Methyl Ether. Many of the participants in Scheme 1 (taking into account also the transition states) are too large to be treated by the CBS-QB3 or G3(MP2) procedures (with our processors); accordingly, we calculated the energetics of these reactions at the density functional B3PW91/6-311G(3df,2pd) level. This functional combination is known to be effective for obtaining ΔH[27,28] and has the advantage that the PW91 correlation correction[29] is the one used by Becke in parametrizing his B3 hybrid.[30] Since the zero-point and thermal contributions to H(298 K) require that the vibration frequencies be determined, which is very time-consuming, we did this with the smaller 6-31G(d) basis set. In seven test cases, we found that the maximum effect upon ΔH(298 K) was only 0.49 kcal/mol. All energy minima and transition states were

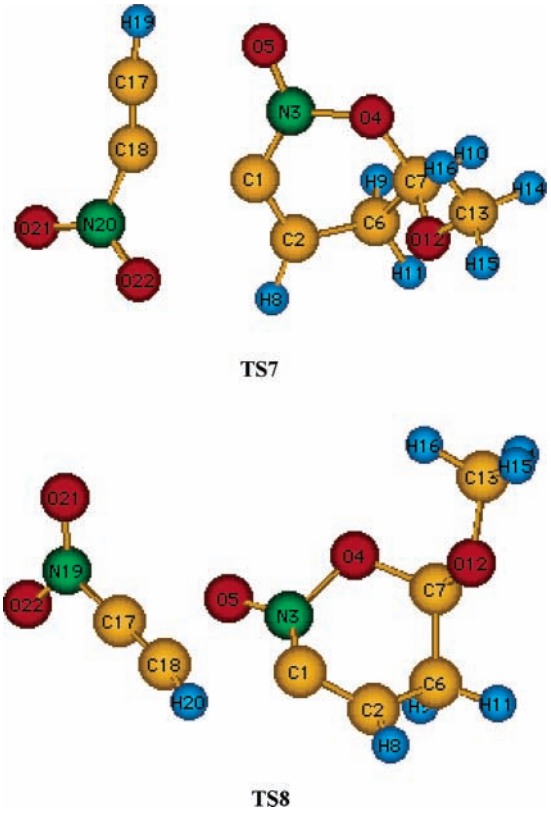

Figure 4. Computed B3PW91/6-311G(3df,2pd) structures of transition states **TS7** and **TS8**. The distances between the atoms forming bonds are as follows. **TS7**: $O_5 \cdots C_{17}$, 2.603 Å; $C_1 \cdots C_{18}$, 2.331 Å. **TS8**: $O_5 \cdots C_{17}$, 2.690 Å; $C_1 \cdots C_{18}$, 2.383 Å.

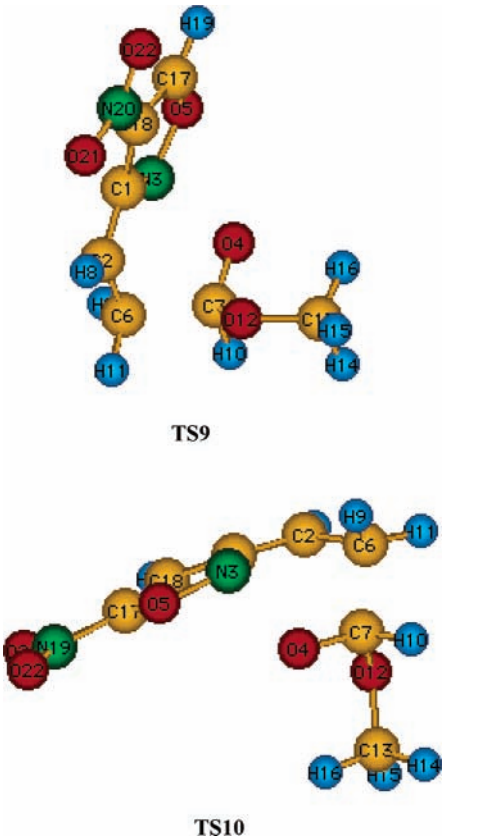

Figure 5. Computed B3PW91/6-311G(3df,2pd) structures of transition states **TS9** and **TS10**. The separations of the atoms between which bonds are being broken are as follows. **TS9**: $N_3 \cdots O_4$, 1.876 Å; $C_6 \cdots C_7$, 1.633 Å. **TS10**: $N_3 \cdots O_4$, 1.874 Å; $C_6 \cdots C_7$, 1.633 Å.

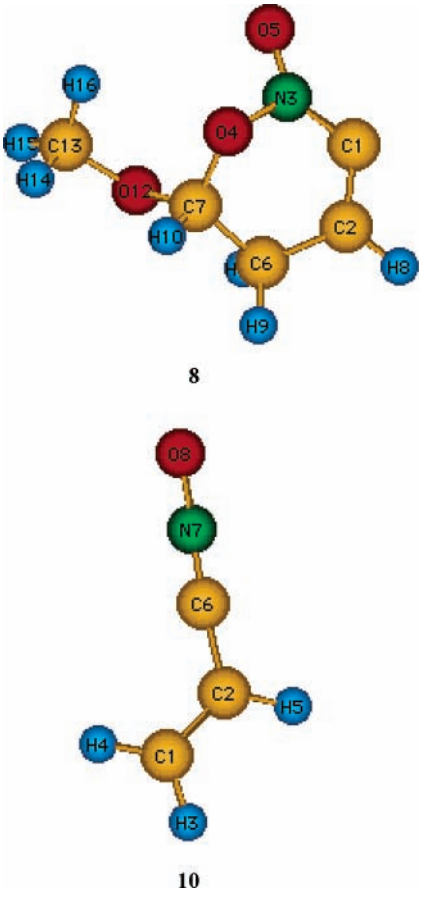

Figure 6. Computed B3PW91/6-311G(3df,2pd) structures of intermediates **8** and **10**. Some key bond lengths and angles are as follows. **8**: C_1-C_2, 1.331 Å; C_2-C_6, 1.490 Å; C_6-C_7, 1.554 Å; O_4-C_7, 1.428 Å; N_3-O_4, 1.469 Å; C_1-N_3, 1.315 Å; N_3-O_5, 1.198 Å; C_7-O_{12}, 1.384 Å; $C_1-N_3-O_4$, 112°; $C_1-C_2-C_6$, 118°; $C_1-N_3-O_5$, 133°; $C_2-C_1-N_3$, 120°; $N_3-O_4-C_7$, 107°. **10**: C_1-C_2, 1.334 Å; C_2-C_6, 1.414 Å; C_6-N_7, 1.160 Å; N_7-O_8, 1.197 Å; $C_1-C_2-C_6$, 124°; $C_2-C_6-N_7$, 174°; $C_6-N_7-O_8$, 179°.

confirmed by verifying that they have zero and one imaginary frequencies, respectively,[31] and in some instances by determining the intrinsic reaction coordinate (IRC).[7]

In Table 1 are presented the computed energies and enthalpies relevant to Scheme 1, including those for the transition states. These data were used to find the heats of reaction, ΔH, and activation barriers, ΔH_{act}, that are given in Table 2. The transition states are shown in Figures 2−5; they all correspond to concerted reactions.

The reactions in Scheme 1 involve three pairs of structural isomers: **6a** and **6b**, **11a** and **11b**, and **12a** and **12b**. Within each of these pairs, the first is the more stable at 298 K, by 2.8, 1.5, and 4.2 kcal/mol, respectively (Table 1). The activation barriers for the formation or reaction of each isomeric pair are quite similar, differing by no more than 2.1 kcal/mol (Table 2).

For the process that we have investigated, nitroacetylene reacting with vinyl methyl ether (**7**), our calculations clearly support the mechanisms proposed by Zhang et al.[1] All of the steps are predicted to be exothermic, and all of the activation barriers, low (<14 kcal/mol).

As expected,[1] **8** fragments readily, with ΔH_{act} being only 5 kcal/mol. Its optimized structure, in Figure 6, supports the depiction (Scheme 1) in which it has adjacent C═C and C═N double bonds; the 1.331 Å C_1-C_2 distance is typical of a C═C double bond, while the C_1-N_3, N_3-O_4, and N_3-O_5 bond lengths are similar to the corresponding ones observed in furoxan

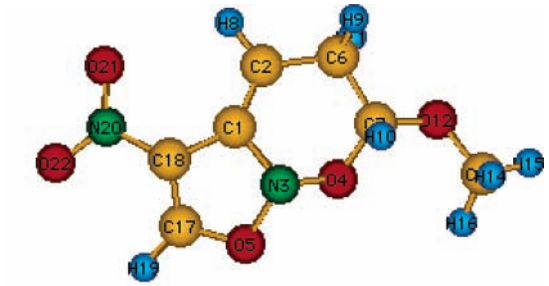

12a

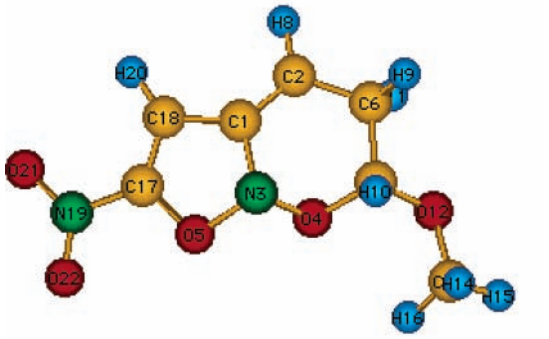

12b

Figure 7. Computed B3PW91/6-311G(3df,2pd) structures of intermediates **12a** and **12b**. For **12a**, some key bond lengths and angles are as follows: C_1-C_2, 1.331 Å; C_2-C_6, 1.500 Å; C_6-C_7, 1.525 Å; O_4-C_7, 1.453 Å; N_3-O_4, 1.402 Å; C_1-N_3, 1.440 Å; N_3-O_5, 1.438 Å; O_5-C_{17}, 1.329 Å; $C_{17}-C_{18}$, 1.347 Å; $C_{18}-N_{20}$, 1.421 Å; $C_1-C_2-C_6$, 121°; $C_2-C_6-C_7$, 112°; $O_4-C_7-C_6$, 110°; $N_3-O_4-C_7$, 104°; $C_1-N_3-O_4$, 109°; $C_2-C_1-N_3$, 119°; $C_1-C_{18}-C_{17}$, 108°; $O_5-C_{17}-C_{18}$, 113°; $N_3-O_5-C_{17}$, 106°; $N_3-C_1-C_{18}$, 103°. The values for **12b** are very similar to the corresponding ones for **12a**.

(**13**).[19] The adjacent double bonds at an angle of 120° would presumably introduce strain, facilitating the fragmentation of the ring in **8**. This produces the vinyl nitrile oxide **10**, also shown in Figure 6. The computed structure of **10** indicates that it is best represented in terms of a C≡N triple bond (Scheme 1);[19] for example, the 1.414 Å C_2-C_6 distance is very close to the 1.427 Å distance of the analogous C—C bond in TCNQ (tetracyanoquinodimethane, **14**).

13 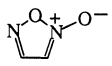

14 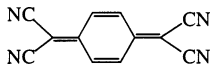

Even more favored kinetically than the fragmentation of **8**, however, is the alternative route whereby **8** adds to **1** and the adducts (**12a** and **12b**) then lose **9** to produce the nitrovinylisoxazoles **6a** and **6b**; the additions are almost barrier-free (<2 kcal/mol), and the loss of **9** has $\Delta H_{act} < 7$ kcal/mol. (The optimized geometries of **12a** and **12b** are in Figure 7.) Since the first steps in both pathways, **8** → **9** + **10** and **8** + **1** → **12a** and **12b**, have very low barriers, $\Delta H_{act} < 5$ kcal/mol, it can be anticipated that both routes to **6a** and **6b** will be followed.

4. Summary

Our analysis has confirmed the feasibility of the mechanisms proposed by Zhang et al. to explain the seemingly anomalous reactions of nitroacetylene with vinyl ethers.[1] It seems likely that both of their suggested pathways are followed. As Zhang et al. point out, the mechanism proceeding through the vinyl nitrile oxide **10** can be extended to the reaction of nitroacetylene with furan.

The electron-deficient nature of the triple bond in nitroacetylene, predicted by Zhang et al.,[1] has been verified by means of the computed molecular surface electrostatic potential, which also shows the characteristic buildup of positive potential above the $C-NO_2$ bond. Finally, to further characterize the structure and properties of nitroacetylene, its calculated molecular geometry and gas and liquid phase heats of formation are presented.

Acknowledgment. We greatly appreciate the support of the Office of Naval Research, Contract No. N00014-99-1-0393, and Project Officer Dr. Judah M. Goldwasser.

References and Notes

(1) Zhang, M.-X.; Eaton, P. E.; Steele, I.; Gilardi, R. *Synthesis* **2002**, 2013.
(2) Alster, J.; Iyer, S.; Sandus, O. In *Chemistry and Physics of Energetic Materials*; Bulusu, S. N., Ed.; Kluwer: Dordrecht, The Netherlands, 1990; Chapter 28.
(3) Politzer, P.; Lane, P.; Wiener, J. J. M. In *Carbocyclic and Heterocyclic Cage Compounds and Their Building Blocks*; Laali, K. K., Ed.; JAI Press: Stamford, CT, 1999; p 73.
(4) Eaton, P. E.; Gilardi, R. L.; Zhang, M.-X. *Adv. Mater. (Weinheim, Ger.)* **2000**, *12*, 1143.
(5) Zhang, M.-X.; Eaton, P. E.; Gilardi, R. *Angew. Chem., Int. Ed.* **2000**, *39*, 401.
(6) Denmark, S. E.; Thorarensen, A. *Chem. Rev.* **1996**, *96*, 137.
(7) Frisch, M. J.; Trucks, G. W.; Schlegel, H. B.; Scuseria, G. E.; Robb, M. A.; Cheeseman, J. R.; Zakrezewski, V. G.; Montgomery, J. A.; Stratmann, R. E.; Burant, J. C.; Dappich, S.; Millam, J. M.; Daniels, A. D.; Kudin, K. N.; Strain, M. C.; Farkas, O.; Tomasi, J.; Barone, V.; Cossi, M.; Cammi, R.; Mennucci, B.; Pomelli, C.; Adamo, C.; Clifford, S.; Ochterski, J.; Petersson, G.; Aayala, P. Y.; Cui, Q.; Morokuma, K.; Malick, D. K.; Rubuck, A. D.; Raghavachari, K.; Foresman, J. B.; Cioslowski, J.; Ortiz, J. V.; Stefanov, B. B.; Liu, G.; Liashenko, A.; Piskorz, P.; Komaromi, I.; Gomperts, R.; Martin, R. L.; Fox, D. J.; Keith, T.; Al-Laham, M. A.; Peng, C. Y.; Nanayakkara, A.; Gonzalez, C.; Challacombe, M.; Gill, P. M. W.; Johnson, B. G.; Chen, W.; Wong, M. W.; Andres, J. L.; Head-Gordon, M.; Replogle, E. S.; Pople, J. A. *Gaussian 98*, revision A.7; Gaussian, Inc.: Pittsburgh, PA, 1998.
(8) Montgomery, J. A., Jr.; Frisch, M. J.; Ochterski, J. W.; Petersson, G. A. *J. Chem. Phys.* **1999**, *110*, 2822.
(9) Curtiss, L. A.; Redfern, P. C.; Raghavachari, K.; Rassolov, V.; Pople, J. A. *J. Chem. Phys.* **1999**, *110*, 4703.
(10) Mallard, W. G., Linstrom, P. J., Eds. *NIST Chemistry Webbook, NIST Standard Reference Database No. 69*; NIST: Gaithersburg, MD, 1998 (http://webbook.nist.gov).
(11) Murray, J. S.; Politzer, P. In *Quantitative Treatments of Solute/Solvent Interactions*; Murray, J. S., Politzer, P., Eds.; Elsevier: Amsterdam, The Netherlands, 1994; Chapter 8.
(12) Murray, J. S.; Brinck, T.; Lane, P.; Paulsen, K.; Politzer, P. *THEOCHEM* **1994**, *307*, 55.
(13) Murray, J. S.; Politzer, P. *THEOCHEM* **1998**, *425*, 107.
(14) Politzer, P.; Murray, J. S. *Trends Chem. Phys.* **1999**, *7*, 157.
(15) Politzer, P.; Murray, J. S. *Fluid Phase Equilib.* **2001**, *185*, 129.
(16) Bader, R. F. W.; Carroll, M. T.; Cheeseman, J. R.; Chang, C. *J. Am. Chem. Soc.* **1987**, *109*, 7968.
(17) Rice, B. M.; Pai, S. V.; Hare, J. *Combust. Flame* **1999**, *118*, 445.
(18) Sadova, N. I.; Vilkov, L. V. *Russ. Chem. Rev.* **1982**, *51*, 87.
(19) Allen, F. H.; Kennard, O.; Watson, D. G.; Brammer, L.; Orpen, A. G.; Taylor, R. *J. Chem. Soc., Perkin Trans. 2* **1987**, S1.
(20) Wilson, E. B., Jr. *Tetrahedron* **1962**, *17*, 191.
(21) Politzer, P.; Harris, R. R. *Tetrahedron* **1971**, *27*, 1567.
(22) Politzer, P.; Bar-Adon, R. *J. Am. Chem. Soc.* **1987**, *109*, 3529.
(23) Murray, J. S.; Lane, P.; Politzer, P. *THEOCHEM* **1990**, *209*, 163.
(24) Politzer, P.; Murray, J. S. In *Reviews in Computational Chemistry*; Lipkowitz, K. B., Boyd, D. B., Eds.; VCH Publishers: New York, 1991; Vol. II, Chapter 7.
(25) Politzer, P.; Murray, J. S. *J. Mol. Struct.* **1996**, *376*, 419.
(26) Politzer, P.; Laurence, P. R.; Abrahmsen, L.; Zilles, B. A.; Sjoberg, P. *Chem. Phys. Lett.* **1984**, *111*, 75.
(27) Sicre, J. E.; Cobos, C. J. *THEOCHEM* **2003**, *620*, 215.
(28) Ventura, O. N.; Kieninger, M.; Denis, P. A. *J. Phys. Chem. A* **2003**, *107*, 518.
(29) Perdew, J. P.; Chevary, J. A.; Vosko, S. H.; Jackson, K. A.; Pederson, M. R.; Singh, D. J.; Fiolhais, C. *Phys. Rev. B* **1992**, *46*, 6671.
(30) Becke, A. D. *J. Chem. Phys.* **1993**, *98*, 5648.
(31) Hehre, W. J.; Radom, L.; Schleyer, P. v. R.; Pople, J. A. *Ab Initio Molecular Orbital Theory*; Wiley-Interscience: New York, 1986.